8-15-2017

# Sensitivity Analysis for Best-Estimate Thermal Models of Vertical Dry Cask Storage Systems

Remy R. DeVoe
*University of Tennessee, Knoxville*

Kevin R. Robb
*Oak Ridge National Laboratory*, robbkr@ornl.gov

Steven Skutnik
*University of Tennessee, Knoxville*, sskutnik@utk.edu



## Recommended Citation

Remy R. DeVoe, Kevin R. Robb, Steven E. Skutnik, "Sensitivity analysis for best-estimate thermal models of vertical dry cask storage systems," Nuclear Engineering and Design, Volume 320, 2017, Pages 282-297, ISSN 0029-5493

# Sensitivity Analysis for Best-Estimate Thermal Models of Vertical Dry Cask Storage Systems

Remy R. DeVoe[a], Kevin R. Robb[b], Steven E. Skutnik[a,*]

[a] *Department of Nuclear Engineering, University of Tennessee-Knoxville, 37996*
[b] *Oak Ridge National Laboratory, 1 Bethel Valley Road, Oak Ridge, TN 37831*

**Abstract**

Loading requirements for dry cask storage of spent nuclear fuel are driven primarily by decay heat capacity limitations, which themselves are determined through recommended limits on peak cladding temperature within the cask. This study examines the relative sensitivity of peak material temperatures within the cask to parameters that influence both the stored fuel residual decay heat as well as heat removal mechanisms. These parameters include the detailed reactor operating history parameters (e.g., soluble boron concentrations and the presence of burnable poisons) as well as factors that influence heat removal, including non-dominant processes (such as conduction from the fuel basket to the canister and radiation within the canister)

*Corresponding author

*Email addresses:* rdevoe1@utk.edu (Remy R. DeVoe), robbkr@ornl.gov (Kevin R. Robb), sskutnik@utk.edu (Steven E. Skutnik)

and ambient environmental conditions. By examining the factors that drive heat removal from the cask alongside well-understood factors that drive decay heat, it is therefore possible to make a contextual analysis of the most important parameters to evaluation of peak material temperatures within the cask.

The goal of this analysis is to afford modelers the ability to develop best-estimate thermal models for vertical dry cask storage systems useful for material degradation studies. In contrast to more conservative bounding analyses used for safety and licensing studies (which are primarily intended to illustrate that recommended temperature limits are not exceeded), material degradation phenomena are frequently temperature-dependent, requiring best-estimate thermal models to properly evaluate.

The canister-level parameters that have the greatest impact on peak fuel material temperatures drive convective heat transfer in the cask annulus (comprised of the region between the storage canister and the concrete overpack) and within the canister basket. These parameters include the ambient air temperature, the canister fill gas pressure, and the pressure drop between the annular region inlet and outlet. Other cask design parameters which would be expected to contribute substantially to the peak clad temperature were overall proved to be of marginal significance, including material properties such as the fuel basket thermal conductivity and emissivity, along with frictional flow losses from the spacer grid. Meanwhile, factors that drive conduction from the fuel basket region and material properties which drive radiative transport between the fuel and basket likewise exhibit low sensitivity for peak clad temperature estimates.

Fuel irradiation history parameters that drive decay heat (such as the discharge burnup and average moderator density) nevertheless dominate peak clad temperature sensitivity. While the assembly power history significantly influences short-term decay heat post-discharge, it manifests minimal sensitivity for cooling times over 10 years and is thus of negligible importance for assemblies stored in wet storage for at least this time.
*Keywords:* COBRA-SFS, Dry Cask Storage, Used Nuclear Fuel, Peak Clad Temperature, Sensitivity Analysis

---

## 1. Introduction

Current thermal analyses for certification of dry cask systems are typically conducted to determine if peak material temperatures remain below recommended limits during normal and off-normal conditions (Office of Nuclear Material Safety and Safeguards, 2010). Because of uncertainties in the cask design parameters and reactor operating history, conservative assumptions are used to create thermal models which bound an envelope of fuel design and reactor operating histories for safety analyses. However, bounding hot models used for safety-related analyses may be unsuitable for material degradation studies that use thermal attributes other than peak material temperatures. For example, safety-related evaluations are typically designed to verify that peak material temperatures will not exceed recommended limits, whereas material degradation studies (such as evaluation of the ductile-to-brittle transition) are interested in the evolution of the clad temperature profile over time, rather than simply the maximum possible clad temperature, wherein material degradation phenomena are often strongly temperature-dependent.

Hence, realistic temperature predictions derived from best-estimate thermal models (which attempt to achieve maximum fidelity of material temperatures within the cask with minimal conservatism, in contrast to standard bounding analyses) are valuable in understanding whether the conditions are sufficient for spent fuel cladding phenomena such as hydride reorientation (occurring as a result of high temperatures and hoop stress) and the ductile-to-brittle transition temperature (occurring at low temperatures) (Sorenson and Hanson, 2013). This in turn helps us understand the susceptibility of cladding to brittle failure in long-term storage conditions (Daum et al., 2006, Kim et al., 2015, Kook et al., 2013).

Hydride reorientation is particularly sensitive to clad temperature (Singh et al., 2006, Min et al., 2014) and internal rod pressure (Cha et al., 2015), including effects introduced by temperature cycling (Chu et al., 2008) and cool-down rates (Min et al., 2014, Cha et al., 2015, Colas et al., 2013, Won et al., 2014), with samples taken with lower cool-down rates showing a higher fraction of radial hydride orientation (Min et al., 2014, Cha et al., 2015), which may contribute to brittle failure. Hydride reorientation is particularly associated with high stress within the clad (such as from internal rod pressure from fission gas buildup, which is proportional to fuel burnup) during cool-down (Valance and Bertsch, 2015). Meanwhile, as the cladding cools, dissolved hydrogen driven into solution will eventually re-precipitate, with a larger fraction re-precipitating at lower cool-down rates (Min et al., 2014). At sufficiently low temperatures (around 200°C), nearly all of the dissolved hydrogen re-precipitates, potentially inducing embrittlement from radial-oriented hydrides within the zirconium (Daum et al., 2006, Billone et al., 2011), referred

to as the ductile-to-brittle transition temperature (DBTT).

Best-estimate thermal models may therefore provide greater insight into predicted peak clad temperatures and cool-down rates as compared to more conservative bounding analyses, given that they attempt to more realistically portray the evolution of clad temperature over time. In particular, such models are essential to understanding phenomena such as DBTT, given that the conservatism employed in bounding models may overestimate clad temperatures over time, thereby potentially overestimating the storage time at which the DBTT threshold is reached within the canister. Crediting realistic assumptions for these parameters has proven challenging because of the experimental measurements and site-specific data required to justify using less bounding values. In as much, establishing the relative sensitivity of peak clad temperature to these parameters is important to characterizing uncertainties inherent in best-estimate thermal models.

In this study we quantify the relative sensitivity of the peak clad temperature (PCT) to each of the above parameters for a vertical dry cask storage system using a best-estimate thermal model of the MAGNASTOR® Transportable Storage Container (TSC-37) (NAC International, 2015) as the basis for this evaluation, with the goal of identifying the most sensitive parameters for vertical spent fuel storage cask thermal models. The most significant sensitivities will have the greatest impact on fuel cladding temperature predictions. PCT was chosen as the sensitivity metric due to both its proportionality to other material temperatures as well as the fact that PCT is used for degradation studies of fuel cladding. Identifying the relative sensitivity of the peak clad temperature to different cask and fuel parameters allows for

modelers to capture the effect of parameter uncertainties in thermal models, thereby potentially reducing conservatism in models attributable to parameters with high-uncertainty but exhibiting low sensitivity, while safely omitting parameters of relatively limited consequence for thermal studies. Here, the sensitivity of peak clad temperature to model parameters is expressed in terms of the *parameter sensitivity coefficient*, defined as the relative change in peak clad temperature (in percent) from that of the nominal model evaluation as a function of the relative perturbation of a parameter value (also in percent) from its nominal value.

For this study, the parameter set investigated includes both cask design features (e.g., material and mechanical properties of the cask that influence heat rejection, including features such as the thermal conductivity and emissivity of canister materials as well as mechanical features such as the pressure drop over the convective surface), environmental factors (such as ambient air temperature and insolation rates), and factors that contribute to the decay heat emitted by the stored fuel (such as burnup, moderator density, and other fuel irradiation history parameters). While the relationship of the decay heat from spent fuel to parameters such as burnup is generally well-known, the goal of this study is to contextualize the sensitivity of factors such as burnup relative to other system-level parameters to afford modelers the ability to understand their relative sensitivity within a unified context. This in turn allows for analysts to focus on quantifying the effect of uncertainties on the most sensitive parameters for dry cask storage systems while placing lower priority on high-uncertainty / low-sensitivity parameters (which have little effect on material temperatures). Similarly, a quantification of the sensitiv-

ity of relevant environmental factors (e.g., ambient temperature, insolation) allows analysts the ability to evaluate how inherent variability owing to environmental factors unique to the canister storage location contribute to overall uncertainties in material temperatures.

Taken together, the above sensitivity coefficient information can be leveraged to further develop best-estimate thermal models for vertical dry cask storage systems and to better understand uncertainties in material temperature predictions arising from these models. (The reader is cautioned however that given the the drastically different heat removal pathways of horizontal dry cask storage systems, the conclusions from this study cannot be directly applied to these systems, which would require a separate sensitivity study.)

## 2. Method

The goal of this study is to characterize the relative sensitivity of all relevant parameters which contribute to the peak clad temperature within the storage cask in order to aid in the development of best-estimate cask thermal models. This includes evaluation of the relative sensitivity of peak clad temperature to each of the various cask, assembly, and environmental conditions inherent to dry cask storage systems, such to allow modelers the ability to prioritize understanding of high-sensitivity parameters (for minimizing model uncertainties) while reducing emphasis on low-importance parameters (which have minimal consequence for clad temperature estimates).

This sensitivity study consists of two thrusts which comprise the dry cask storage system: the factors which contribute to the spent fuel decay heat source term itself (i.e., the assembly design and irradiation history parame-

ters) along with the cask design and environmental factors which influence the heat removal rate from the canister. While the relationship of assembly decay heat to burnup is generally well-known, a key focus of this analysis is presenting the sensitivity of these parameters within the context of a dry cask storage system in order to afford a direct comparison of the most important assembly and cask design parameters for determining in-cask clad temperatures in best-estimate thermal models.

The first objective was to evaluate the sensitivity of decay heat to fuel depletion parameters. The effect of assumptions used in lattice physics models to generate cross-section libraries is quantified by varying these parameters using data from previous criticality studies and in-core instrumentation. The second study focused on the sensitivity of the cask thermal model to cask design and environmental parameters.

Because of the frequently proprietary nature of many of the most important cask and fuel history parameters, combined with inherently variable site-specific features (e.g., ambient temperature, insolation, etc.), cask geometry and boundary conditions used for thermal models must often be approximated. To afford a characterization of the most sensitive parameters for cask thermal studies, both studies therefore used the same best-estimate dry cask thermal model to allow a comparison of each parameter and establish a rank ordering based on their impact on material temperatures over time.

The sensitivity analysis presented here encompasses commercial pressurized water reactor (PWR) fuel and vertical cask characteristics used to create thermal models, which draws extensively upon analysis tools developed for

performing PWR assembly burnup credit studies. Though the cask design is for PWR fuel, vertical cask systems designed for BWR fuel share many similar characteristics. However, BWR assemblies present the additional degrees of freedom in the analysis of the assembly decay heat (e.g., axial void profiles, variable pin enrichments, etc.) which are not explored in this analysis. Meanwhile, the findings of the study are applicable only to vertical dry cask storage systems, as horizontal dry cask storage systems rely on significantly different heat removal mechanisms.

### *2.1. Analysis Codes*

This sensitivity study was performed using the same analysis codes and models currently in use for evaluating cask temperatures using best-estimate modeling practices (Scaglione et al., 2014, Robb et al., 2014). Each code has been validated for this specific task, and the best-estimate thermal models were verified against results reported in the final safety analysis report (FSAR) for each licensed cask design. The lattice physics and depletion models were made using modules in the SCALE 6.2 public beta release (version 4) developed by Oak Ridge National Laboratory (Bowman, 2011). The dry cask thermal hydraulics models were made using the well known dry cask thermal hydraulics code Coolant Boiling in Rod Arrays–Spent Fuel Systems (COBRA-SFS) version 4 developed by Pacific Northwest National Laboratory (Michener et al., 2015).

#### *2.1.1. SCALE*

The SCALE code system is used to generate fuel design and reactor-specific cross section libraries to deplete fuel and generate isotopic compo-

sition and decay heat source terms. The TRITON control module was developed to perform light water reactor lattice physics calculations and was used in this study to generate burnup-dependent cross-section libraries (DeHart and Bowman, 2011). ORIGEN was used to perform point depletion and decay calculations to obtain decay heat source terms for the sensitivity study (Gauld et al., 2011). Both TRITON and ORIGEN have been validated against over 160 calorimetric measurements of decay heat data from commercial spent fuel assemblies (Gauld et al., 2010, Radulescu et al., 2010).

ORIGEN's new ORIGAMI interface (available with the SCALE 6.2 release) is used in this study to rapidly analyze commercial spent fuel decay heat source terms. ORIGAMI is a flexible, easy-to-use system developed specifically for characterizing commercial spent nuclear fuel (Skutnik et al., 2015). ORIGAMI is designed to evaluate depletion of nuclear fuel assemblies with axial and radial burnup gradients, performing point depletion calculations using ORIGEN based upon the user-supplied power shaping mesh. The ORIGAMI interface leverages the recently modernized ORIGEN API to provide a convenient interface for assembly-level ORIGEN calculations (Skutnik et al., 2013, Wieselquist, 2015); thus, ORIGAMI relies on the same validated methods and data as ORIGEN. Here, ORIGAMI is particularly useful for its ability to define each pin and axial zone with specific cross-section libraries as needed in order to capture variations in the local neutron spectra, owing to changes in fuel burnup, moderator density, and pin enrichments present within commercial reactor fuel through a single, simplified input file.

For the depletion analysis performed in this study, a uniform radial power map was applied for each axial zone while individual region-specific libraries

were used for each pin to capture local variations in the neutron spectrum (e.g., proximity to guide tubes, absorber rods, etc.). Meanwhile, an axial power gradient was employed over the length of the assembly, resulting in a different average power/burnup for each axial zone (while preserving the assembly-average power and burnup).

#### *2.1.2. COBRA-SFS*

COBRA-SFS is a single-phase sub-channel analysis code tailored to provide a multi-dimensional finite-difference solution for heat conduction and convection in dry casks for both steady-state calculations and transients. Originally developed in 1986, COBRA-SFS can calculate material temperature predictions for complex geometry multi-assembly cask systems. COBRA-SFS is used by the NRC to verify that dry cask designs meet thermal performance requirements during normal and off-normal storage scenarios (Adkins Jr. et al., 2009). The COBRA-SFS code system was selected for best-estimate thermal analysis over a computational fluid dynamics (CFD) approach because sub-channel analysis codes have much shorter run times (usually on the order of hours for a full cask system compared to the days or weeks required to achieve comparable results using CFD) (Bajwa and Spivack, 2007).

### *2.2. Sensitivity Calculation*

In the course of this study, we identified a number of parameters that were either highly variable or unknown without physical measurements. We therefore performed this sensitivity study by incrementally varying each parameter from the nominal value used in the best-estimate model within an

interval of what is reasonably expected in actual cask systems. A steady-state simulation was run using each unique model to measure the response in peak cladding temperature.

Each parameter has a characteristic impact on cask materials, and this impact is measured using the PCT. One simple method to rank parameters from least to greatest importance is to use the maximum change in PCT. While this method can be used to compare the change in PCT based on the maximum uncertainty in each parameter, it does not measure how material temperatures change with small variations from the nominal value. A more preferable method is used to rank parameters by calculating the differential change in PCT due to a differential change in the modeling parameter. This produces a rate value (known as the sensitivity coefficient) for each parameter. Sensitivity coefficients are calculated using Eqn. 1, where $a_i$ is the fuel or cask parameter being studied. Here, the sensitivity coefficient $\frac{\delta T_{PCT}}{\delta a_i}$ represents the relative magnitude of the PCT response to a relative change in the parameter of interest, $\Delta a_i$.

$$\Delta T_{PCT} = \left( \frac{\delta T_{PCT}}{\delta a_i} \right) \Delta a_i \tag{1}$$

Implicit in Equation 1 is the assumption that each parameter value has a linear and independent relationship with PCT such that changing one parameter has no impact on other parameters.

The best-estimate model is used as the baseline for comparison between each model. The percentage change in PCT ($\Delta T_{PCT}$) and each parameter ($\Delta a_i$) is calculated relative to the nominal value used in the best-estimate model and the resulting PCT. The percentage change in PCT for each model

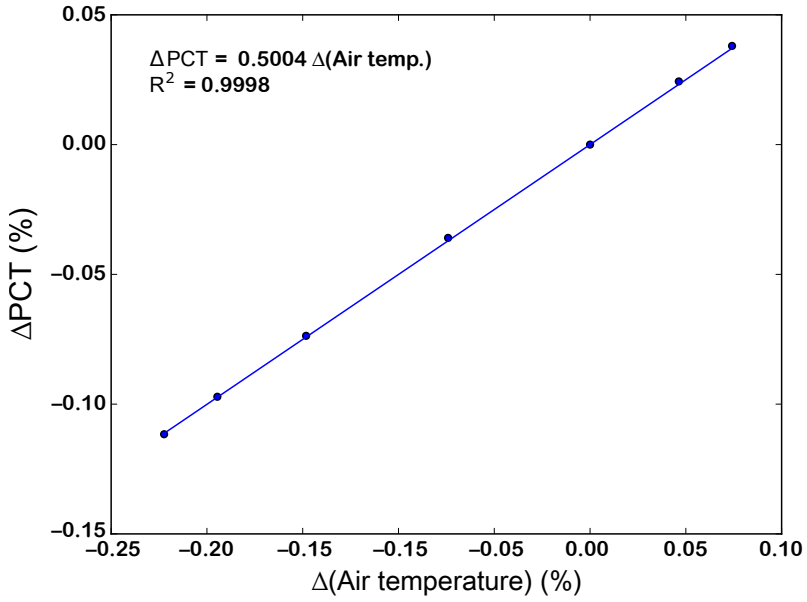


Figure 1: Linear least-squares regression for the PCT sensitivity coefficient for ambient air temperature; $\Delta_{PCT} = 0.5004\Delta T_{air}$, $R^2 = 0.9998$

is plotted against the relative change in the parameter being studied, as shown in Fig. 1, and a linear least-squares fit to the data is used to calculate the sensitivity coefficient. The slope of the linear fit to the normalized relative change in the parameter value (in percent) to the change in PCT (also in percent) gives the value of the sensitivity coefficient $\left(\frac{\delta T_{PCT}}{\delta a_i}\right)$; meanwhile, the degree to which an assumption of a linear relationship is appropriate is captured by the coefficient of determination $R^2$, which measures how closely the data is represented by the linear fit. Here, a positive sensitivity coefficient therefore implies an increased PCT with an increasing parameter value and vice versa; likewise, a larger absolute value of the sensitivity coefficient implies greater sensitivity to the parameter in question (i.e., a larger PCT response to a change to the parameter in question).

## 3. Best-Estimate Thermal Model

Before beginning the sensitivity study, a high-fidelity best-estimate model is needed to accurately assess each parameter. This model has the best available data used to create the cask geometry, material properties, and heat transfer correlations as well as assumed nominal values for those parameters used in the sensitivity study. The modeling assumptions were made based on available data and reference material, including thermal analyses in the cask license FSAR (NAC International, 2015). Best-estimate modeling techniques are needed to create the model so that the results of the study can be applied to improving best-estimate models.

The main difference between the models used in this study and the qualifying analyses used for licensing is that fuel assembly geometry is explicitly defined down to the pin level. Typically, thermal analyses done using CFD for licensing require simplifying assumptions to reduce computational complexity and run time. This includes using an equivalent conductivity model that assumes each assembly is a homogeneous solid, neglecting flow in subchannels and radiative heat transfer from pin-to-pin and from pin-to-wall. At every opportunity, the models in this study use actual geometry and material properties when necessary data is available.

The cask system and canister design chosen for the sensitivity study is the MAGNASTOR® Transportable Storage Container (TSC-37) (NAC International, 2015). This canister is designed to accommodate 37 PWR spent fuel assemblies. The MAGNASTOR® cask system is licensed and built by NAC International and is currently in use at Zion, McGuire, and Catawba nuclear power plants (NAC International, 2015). This design was chosen

because it is a representative vertical system similar to other designs, like Holtec International's HI-STORM® 100 system, and others also employed at non-shutdown sites. This type of system is characterized for having fuel stored in a welded canister within a vertical shielded overpack. Spent fuel inventories stored in these types of canister represent over half of all current casks in the U.S. (Greene, 2015).

The thermal model is divided into multiple regions, which employ different methods to solve for material temperatures, as shown in Fig. 2. The majority of the model is within the basket region, which encompasses the whole basket of the canister and extends radially out to the exterior surface of the concrete overpack. Convection and conduction are both calculated in the basket region where the upper and lower plena are treated as one-dimensional conduction regions. The upper and lower plena are defined by the multiple layers of media between the basket region and the respective boundary conditions.

### *3.1. Basket Region*

The basket region is discretized both axially and radially into control volumes further referred to as "nodes." The basket region is created using 47 uniform axial zones; each basket region is discretized using the same nodalization scheme, therefore requiring axial uniformity modeling in the basket region. Fig. 3 shows the nodalization scheme for each fuel tube and labels the materials used in the model. The TSC-37 basket is created from welding 21 fuel tubes together, which create additional developed fuel cells to hold 37 fuel assemblies. Fuel tubes are constructed with carbon steel and modeled as four walls subdivided into 16 nodes, with four nodes at each

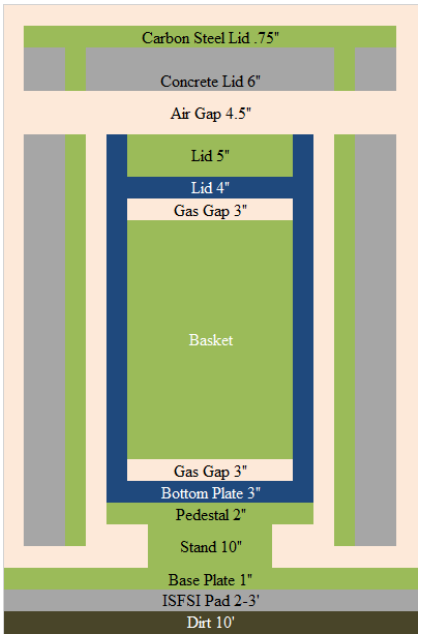


Figure 2: Basket and axial plena in the thermal model (not to scale)

corner. Stainless steel–wrapped neutron absorbers line the inside of each fuel tube, which are divided into four nodes. Conduction between nodes is modeled without any gas gap except between the neutron absorbers, the fuel tube, and stainless steel sheath.

Support plates are welded and bolted around the edge of the basket for structural stability, as shown in Fig. 4. Plates in contact with fuel tubes are subdivided so that node edges in the fuel tubes match those of the support structure. Some basket nodes are in contact with the stainless steel canister, which is subdivided into 16 azimuthal segments that are each divided into two nodes, radially. The canister is centered within the cask annulus, resting on the pedestal of carbon steel. Within the annulus are carbon steel shims welded to the inner liner of the overpack to prevent the canister from shifting

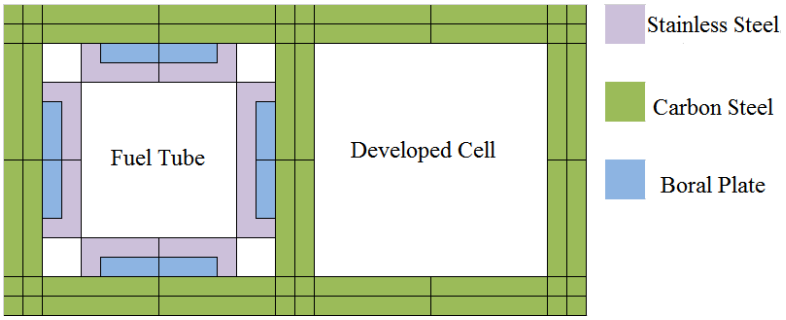


Figure 3: Nodal representation of fuel tubes (not to scale)

within the overpack. The concrete overpack is modeled as equal volume nodes broken up into three radial zones and 16 azimuthal regions. In total there are 1156 nodes per axial zone, creating 54,332 nodes in the entire basket region not including those used in each fuel assembly.

Within the canister geometry, a few edges of the basket structure are in contact with the canister shell, and conduction is modeled between these nodes. Because of thermal expansion and tolerances in the basket design, the gap between the basket structure and canister shell is assumed to be 1/16th of an inch.

COBRA-SFS models are not created with a Computer-Aided Design (CAD) model, like some thermal hydraulics tools, but are instead defined by connections between nodes. Conduction, convection, and radiative heat transfer between nodes is specified with user-calculated connection types. Because of repetition, connection types are created sequentially using characteristic geometry, material properties, and heat transfer correlation. Channels are also connected to other channels and solid nodes to model lateral crossflow and convective heat transfer.

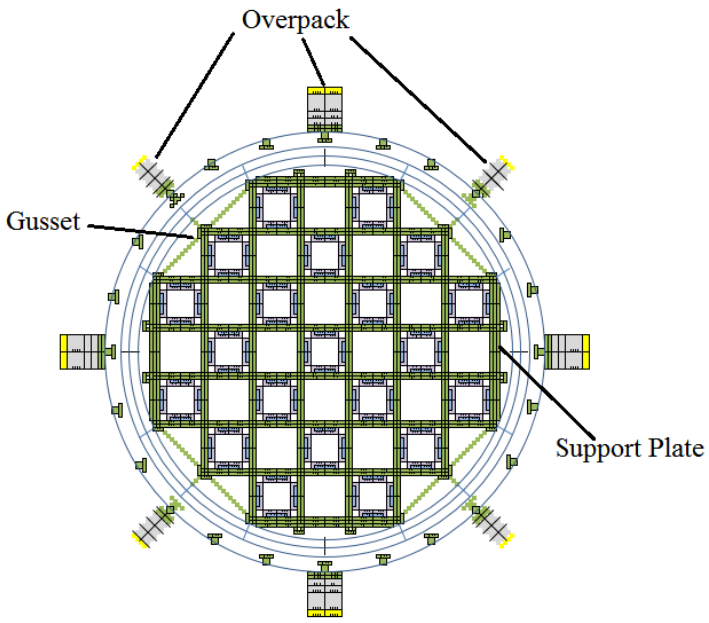


Figure 4: Nodal representation of the basket region

### *3.2. Fuel Modeling*

The fuel design used in the study is the 15 × 15 Westinghouse LOPAR assembly, which is consistent with the spent fuel in dry storage at Zion nuclear power plant. This design uses a 15 by 15 array of 204 fuel rods, each with a diameter of 0.422 inches and a pitch of 0.563 inches, and another 20 guide tube (GT) and 1 instrument tube (IT) positions that are modeled as solid, non-heat generating rods. Only the exterior surface of the cladding (with a constant heat flux at each axial node) is modeled for the steady-state calculations used in this study. Modeling guide tubes and instrument tubes as solid bodies (rather than as void) accounts for the fact that flow is generally constrained through these bodies; the flow is likewise assumed not to interact with the bulk convective flow across the fuel pin. The assumption of no fluid

flow through these rods is therefore a moderately conservative assumption.

As noted previously, the key figure of merit used in the sensitivity study is the PCT. The temperature drop across the cladding thickness is negligible for the heat fluxes considered in this study. Therefore, only the cladding surface temperature is resolved for the following sensitivity study for steady-state conditions. Between fuel rods and the fuel tube walls are 256 sub-channels with convective flow connections defined for each nodal surface. Conduction through spacer grids and upper and lower end-fittings is neglected in the best-estimate model due to restrictions on axial variations in the basket region, but a drag coefficient of 2 is used at each hardware location and 0.5 is used for the fuel tube exit and inlet losses. We employed the RADGEN (Michener et al., 2015) code to calculate the pin-to-pin greybody view factors used to determine radiative heat transfer between pins and the inner surfaces of the fuel tubes.

Decay heat is calculated for each assembly in a depletion model using pre-generated cross-section libraries for each fuel design. The one-group cross sections were produced by the TRITON lattice physics code, using the assembly dimensions in Table 1, for a quarter-symmetry model of the fuel shown in Fig. 5. Each nuclear plant operator reports fuel discharge date, initial enrichment, and burnup, but the operating history and core loading are omitted due to their proprietary nature. These parameters are approximated in depletion and lattice physics models from core loading maps and operating history provided by a few plants for a limited number of cycles (Radulescu et al., 2008).

The axial burnup profile used to model the distribution of decay heat

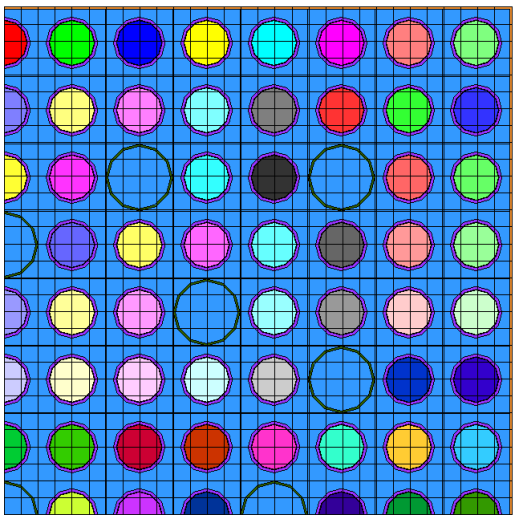

Figure 5: 1/4 model of bounding W1515WL assembly in TRITON; each pin is represented as a separate depletion material to enable pin-specific libraries to be used with ORIGAMI for depletion analysis.

Table 1: W1515WL Fuel Type Specifications

| Assembly Design Data | Values[†] |
|---|---|
| Lattice Pitch (cm) | 21.6163 |
| Rod Pitch (cm) | 1.43002 |
| Pellet Diameter (cm) | 0.929386 |
| Cladding Diameter (cm) | 1.07188 |
| Cladding Thickness (cm) | 0.06172 |
| Cladding Material | Zircaloy-4 |
| GT Diameter (cm) | 1.38684 |
| IT Diameter (cm) | 1.38684 |

[†] taken from (Office of Civilian Radioactive Waste Management, 1987)

axially in each assembly is created by dividing the active fuel region into 18 axial nodes and distributing the assembly irradiation power for depletion calculations (using ORIGAMI) based on a nominal burnup profile; this in turn results in an axial decay heat profile for the assembly used in the thermal

hydraulic analysis using COBRA-SFS. The normalized axial profile shown in Fig. 6 was chosen from the PWR burnup profile database by averaging all the profiles and selecting one that had the lowest residual differences from the average profile (Cacciapouti and Volkinburg, 1997). Note that the assembly design for the selected burnup profile (based on Crystal River 3, Rod H10, a B&W 15×15 assembly with a discharge burnup of 39,749 $\frac{\text{MWd}}{\text{MTU}}$) differs slightly from the design of the nominal assembly design used for the calculations (a Westinghouse 15 × 15 LOPAR assembly); however, the chosen profile more closely approximates the axial profile used in the FSAR compared to available axial power profiles that correspond to the Westinghouse 15×15 design (such as H.B. Robinson Unit 2), which employed axial blankets, leading to a sharper drop-off in the axial power fraction near the assembly edges. Meanwhile, it should be observed that the nominal axial power profile used for the best-estimate thermal model differs slightly from the more approximate profile used for the FSAR analysis. The sensitivity of burnup profile skewness (i.e., the ratio of the relative power fraction in the bottom versus the top of half of the assembly) on PCT is investigated as part of this study.

### *3.3. Boundary Conditions*

The parts of the model that exist outside of the basket region are treated separately by using heat transfer correlations that connect the model to the environment. These include the upper plenum, the lower plenum, and the outer surface of the overpack. Each has its own specific set of boundary conditions owing to the orientation and type of heat transfer occurring. The best-estimate model also includes environmental factors that have a significant impact on material temperatures within the overpack and canister,

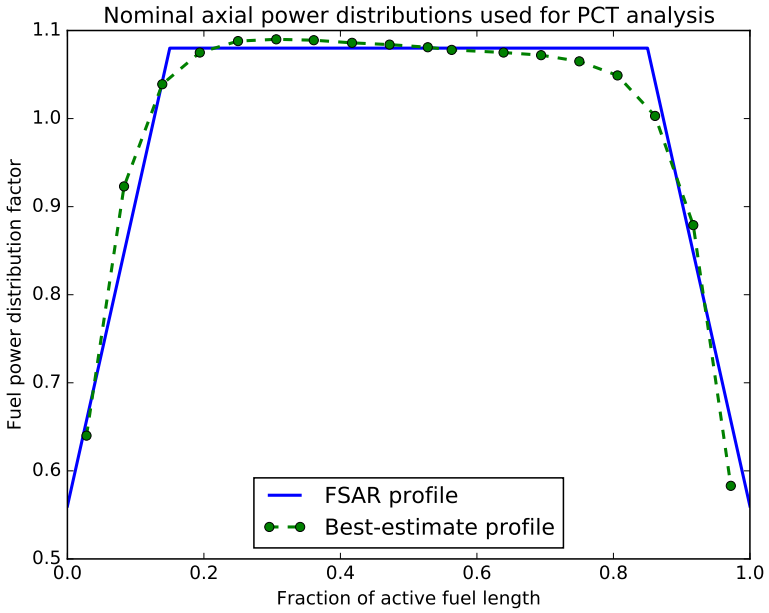


Figure 6: Normalized axial power profiles used for FSAR and best-estimate thermal models; FSAR data adapted from (NAC International, 2015), best-estimate profile based on Crystal River 3, Rod H10 from (Cacciapouti and Volkinburg, 1997).

such as insolation and ambient air temperature. The upper and lower plena are connected to the boundary conditions by a one-dimensional conduction model that uses connection types similar to those used in the basket region to transfer heat through the layers of steel and concrete to the outside environment. The basket region nodes in the canister, overpack, and basket itself are connected to each plenum that contacts or provides ample surface area for radiative heat transfer. The plena modeled in this sensitivity study are shown in Fig. 2.

The top plenum consists of the helium gap (oriented above the fuel basket), which connects to the multi-layered stainless steel canister lid. The canister shell nodes that reside in the basket region of the model are con-

nected to the canister lid in order to model the conduction between the two metals. Above the canister lid is an air gap in the cask annulus that can act as a thermal conductor while also radiating heat across to the bottom surface of the overpack lid. The cask lid is made of concrete, with a cap made of carbon steel, and connects the thermal model to the ambient air above the cask. The bottom plenum is similarly constructed by connecting the basket region to the bottom plate (made of 3-inch-thick stainless steel). Conduction through the fuel assemblies' lower-end fittings and the helium gap is neglected, but the conduction through the corner weld rods in the basket that extend to the bottom plate to support the basket is modeled. The bottom plate rests upon a pedestal in the cask annulus made of carbon steel and air, which is homogenized into one material using the area's averaged conductivity. The pedestal conducts into the baseplate, which connects to 3 feet of ISFSI (Independent Spent Fuel Storage Installation) pad concrete and finally the earth. The far-field ground temperature is assumed to be a constant 40 °F (4.4 °C) as an ultimate heat sink.

The top and sides of the overpack have imposed heat transfer correlations based on natural convection to the ambient air. The carbon steel plate in the overpack lid in the upper plenum uses free convection from a heated horizontal plate facing up to air at 80 °F (26.7 °C). Insolation on the top surface is averaged over a 12 hour period for a boundary heat flux of 387.75 $\frac{\mathrm{W}}{\mathrm{m}^2}$ (122.9 $\frac{\mathrm{Btu}}{\mathrm{h-ft}^2}$) (U.S. Nuclear Regulatory Commission, 2017). The sides of the overpack use free convection from a heated vertical plate to air at 80 °F. Insolation on the sides of the cask is assumed to be half that of the top due to shadowing from the cask itself (U.S. Nuclear Regulatory Commission, 2017).

Natural circulation through the cask annulus is the primary means of heat removal from the canister surface. The flow through the annulus is modeled by solving for air velocity using a user-specified pressure drop between the inlet and exit vents of the overpack. Buoyancy-driven flow is determined by differences in air densities between the ambient air and air in the annulus and by the height difference between the two columns of air (given as Equation 2), similar to a manometer. Friction through the annulus is taken into account from the wetted perimeter specified in the channel definition and the inlet, and exit losses are accounted for in the pressure drop calculation. Per the MAGNASTOR® FSAR, convection-driven flow in the annular region is assumed to be turbulent flow (NAC International, 2015).

$$\Delta P = (\rho g h)_{\text{outside}} + (\rho_{\text{outside}} - \rho_{\text{plenum}})\, g h_{\text{plenum}} - (\text{losses}) \tag{2}$$

Here the reader should note a larger pressure drop over the annular region (due to the change in air density between the outside air and the plenum region at the top of the cask) implies greater buoyancy-driven flow (and therefore, a higher degree of heat removal). Meanwhile, the annulus pressure drop is not fully independent of the ambient air temperature, given that the inlet air density will change by approximately -25% between the bounding cold (-40 °F) and bounding hot (106 °F) ambient temperature conditions.

### *3.4. Model Verification*

To verify that the thermal model is behaving properly and that the results are reliable, a number of test cases were performed to ensure that the model was constructed accurately. This includes simple problems to test solution

stability and also verification models to compare results between accepted code models and the best-estimate model used in this study.

A zero heat test was run using the best-estimate model with the expectation that all material temperatures were the same as the ambient air temperature. For this model, each assembly was modeled with zero decay heat and insolation was neglected, leaving the model to have no heat flux. The ground temperature and the air temperature were both assumed to be 80 °F to create an isothermal system. All material temperatures were within ±0.1°F of the ambient air temperature (assumed to be 80 °F), and the differences were assumed to be from the numerical solver and round-off error.

The verification model was developed to replicate the results of one of the thermal analyses used in the FSAR for storage. The problem involved having a fully-loaded canister containing the maximum heat load during extreme weather conditions. This included modeling the ambient air temperature at -40 °F (-40 °C) and 106 °F (41.1 °C), which represent the extreme lows and highs expected during storage at an ISFSI; these temperatures correspond to the design-basis three-day average extreme temperatures used for the MAGNASTOR® licensing evaluation (NAC International, 2015).

The thermal models used in the FSAR were created using the ANSYS Fluent code and are considerably different from the best-estimate model due to differences between the codes and the added conservatism in the FSAR model for bounding temperature predictions. Rather than treating heat transfer through a pin-level lattice within the fuel basket region, the ANSYS analysis calculates an effective conductivity from a the 2-D lattice, treating the assembly geometry as a porous homogenized cuboid for evaluating heat

transfer (NAC International, 2015). Similarly, the ANSYS model used for the FSAR neglects conduction via the basket stiffeners from the fuel baskets to the canister shell (a conservative assumption), assuming all heat removal from the fuel basket occurs via convection and radiation (NAC International, 2015).

In order to achieve as close as possible correspondence for the validation study presented in Table 2 between the best-estimate model and the FSAR, conduction from the fuel basket region to the canister wall was turned off for the model validation comparison. (Basket-to-canister conduction was enabled for the remainder of the sensitivity study.)

Table 2: Comparison of calculated PCT for the MAGNSTOR FSAR (NAC International, 2015) and the best-estimate validation model developed for this analysis

| Ambient Temperature (°F) | FSAR (°C) | Best-Estimate (°C) |
|---|---|---|
| -40 | 317 | 303.3 |
| 106 | 400 | 387.2 |

Among the observed differences between the best-estimate thermal model and the FSAR analysis (NAC International, 2015), key differences in the analysis include modeling of the fuel geometry as discrete heat-generating rods rather than as homogenized solid with an effective porosity. In addition, the more approximate burnup profile used for the FSAR analysis (shown in Figure 6) may result in a more conservative approximation of PCT, owing to the slightly higher distribution of decay heat toward the top of the assembly; this in turn may explain the relatively consistent difference in PCT observed between the ambient inlet air temperature extrema. Given the close cor-

respondence of the response of PCT to ambient air temperatures over the most likely range of conditions, the best-estimate model appears to show sufficient fidelity from which extrapolative studies on the sensitivities of various modeling assumptions can be conducted.

## 4. Thermal Model Sensitivity

The results presented in this study identify which parameters have a significant impact on material temperatures with the expectation that further investigation or best practices can be developed using this data. The parameter values used in the best-estimate thermal model were chosen based on design data and open literature to provide a means to reasonably predict material temperatures over time. The study investigates the parameters that are used to both generate cross sections in the fuel lattice physics model and to define the geometry and thermodynamic properties within the cask thermal model. The work was divided into two studies to investigate these two areas of best-estimate thermal models. Though two studies were performed, the methods used to obtain sensitivity coefficients for each parameter are such that all parameters can be directly compared and ranked.

### *4.1. Decay Heat Sensitivity*

Cask material temperatures are directly proportional to the total heat loading within the canister. The modeling techniques used to determine total assembly decay heat have been shown to accurately predict total assembly decay heat given detailed reactor history and the fuel design characteristics (Gauld et al., 2010). The sensitivity analysis of depletion modeling parameters quantifies how each parameter used to generate assembly-specific, one-

group cross sections affects decay heat predictions and the corresponding cask temperatures. Each parameter used in the lattice physics model (enumerated in Table 3 is individually varied while all others are held constant to generate a new cross-section library. Decay heat is time-dependent, and the sensitivity of each parameter may also change with decay time—owing to different rates of ingrowth and decay of decay-heat-contributing isotopes. Because of this effect, sensitivity coefficients are calculated at multiple decay times.

Table 3: Lattice physics and depletion parameters used for sensitivity analysis

| Reactor Parameter | Nominal | Minimum | Maximum |
|---|---|---|---|
| Fuel temperature (K) | 1173 | 600 | 1300 |
| Moderator temperature (K) | 579 | 550 | 625 |
| Moderator density ($\frac{g}{cm^3}$) | 0.6668 | 0.6 | 0.75 |
| Soluble boron concentration (ppm) | 1000 | 0 | 2000 |
| WABA | None | None | In |
| Pyrex | None | None | In |
| IFBA | None | None | In |
| Enrichment (wt%) | 2.3 | 1 | 5 |
| Burnup ($\frac{GWd}{MTU}$) | 40 | 38 | 42 |

The reactor design emulated in the lattice physics model is a generic PWR using representative operating parameters listed in Table 3 for a typical reactor running at full power. Some time and spatially-dependent parameters are represented by an average value used to generate the cross-section libraries. For instance, the soluble boron concentration typically starts at the beginning of a cycle with a high value of 2,000 parts per million (ppm), and by the end of cycle the concentration is near zero. The letdown curve of soluble boron is characteristic of the reactor and the core loading, which de-

pends on enrichment, burnup, and burnable poison rod assembly (BPRA) insertion. With respect to this latter condition, multiple burnable absorber types were considered, including integral fuel burnable absorber (IFBA), wet annular burnable absorber rods (WABA), and traditional borosilicate glass (Pyrex) rods. The use of BPRAs is usually reserved for fresh fuel when the fuel has the most excess reactivity. Because BPRA is typically only used in an assembly for the first cycle, the best-estimate cross-section libraries are generated without BPRA. Moderator temperature and density also vary with position in the core but are represented by an average value in the lattice physics model. Each of the sensitivity coefficients are calculated at an assembly average burnup of 40 $\frac{\text{GWd}}{\text{MTU}}$.

Given that the uncertainty in burnup from in-core instrumentation is typically about 5%, this range was used to develop the range of burnups considered for this sensitivity study; a $\pm 5\%$ bound was likewise used to evaluate the sensitivities of the fuel temperature, moderator temperature, and moderator density. The fuel enrichment was evaluated from 1–5% initial $^{235}$U, encompassing the full range of commercial fuel enrichments in the U.S. (Here it should be noted that discharge burnup is typically correlated to initial enrichment; however, for the purposes of this study, the sensitivity of PCT was considered in isolation of burnup.)

For all reactor cycle history sensitivities, the resulting decay heat from a change in the reactor operating parameter is converted to a response in PCT. This is done by varying the assembly's average power in the uniform decay heat loading pattern used in the COBRA-SFS base-case model to multiple power levels and using the resulting change in PCT to derive a correlation

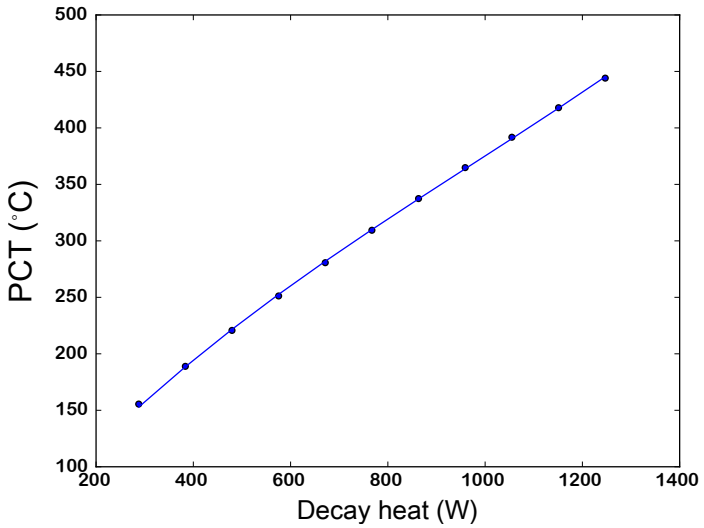


Figure 7: Least-squares regression fit of PCT (in °C) to decay heat; $\mathrm{PCT}\,(q_{decay}) = 7.8 \cdot 10^{-8} \cdot q_{decay}^3 - 2.27 \cdot 10^{-4} \cdot q_{decay}^2 + 0.497 \cdot q_{decay} + 26.7$, with $R^2 = 0.9998$

between assembly average decay heat and PCT, as shown in Fig. 7. The relative sensitivity of each parameter is then determined by performing a linear fit to the relative fractional change in PCT to the change in each modeling parameter; i.e., the slope of this linear fit corresponds to the sensitivity of PCT to the parameter in question.

The lattice physics model sensitivity study showed that most of the nominal reactor operating history values used to generate cross-section libraries have a minimal impact on cask material temperatures. In Fig. 8, each parameter's sensitivity is plotted, and the slope of each line corresponds to the sensitivity of that parameter. Referring back to Equation 1, here the steeper the slope, the greater the parameter sensitivity. Parameters with a positive sensitivity coefficient slope exhibit an increase in PCT with a marginal parameter increase (wherein the steeper the slope, the greater the rate of the

PCT increase), whereas those with a negative slope are negatively correlated with a change in PCT (i.e., increasing the parameter value decreases the PCT).

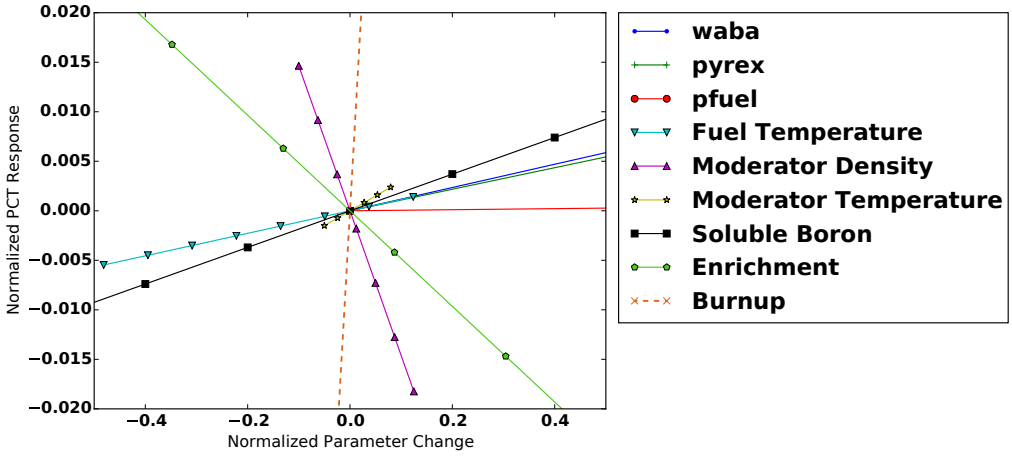


Figure 8: Normalized PCT sensitivity to cycle history parameters after 17 years of cooling time. Note that the burnup perturbation conditions evaluated exceed the ordinate range of the chart, due to the much higher relative sensitivity of burnup compared to other cycle history parameters.

Per Figure 8, the most sensitive fuel parameters for PCT are burnup, moderator density, and enrichment. Here, burnup exhibits a very large positive slope, indicating a high large, positive PCT response in response to increasing burnup. Conversely, moderator density shows a strong negative slope, indicating a higher PCT response for decreasing average moderator density; a similar phenomenon is observed for enrichment. Physically, each of these sensitivities can be understood in the manner in which they impact the decay heat of the stored fuel. Burnup significantly impacts the decay heat given that it is directly proportional to both the number of fissions (impacting significant medium-lived fission product nuclides like $^{137}$Cs and $^{90}$Sr)

as well as neutron captures (driving the longer-lived decay heat source term from the decay of transuranic species). Moderator density determines the neutron energy spectrum, thereby changing the reaction rates for fission and neutron absorption in the fuel, leading to differences in the total decay heat. Enrichment has a similar effect on the fission cross-section in the fuel, which is used to calculate the neutron flux that also contributes to the creation of actinoids from neutron absorption in $^{238}$U.

Differences in isotopic composition and their half-lives can lead to significant variations in sensitivity coefficients over time. The sensitivity coefficients at 17, 50, and 149 years are thus shown in Table 4 along with the maximum difference in PCT for all decay times evaluated. The largest difference in PCT (25 °C) is due to a 5% uncertainty in burnup; burnup likewise exhibits the largest sensitivity coefficient (0.9088) at 17 years of cooling time.

Table 4: Cycle history sensitivity results summary and time-dependent rank ordering of PCT sensitivity to parameters (1 = highest parameter sensitivity). Note that a positive sensitivity coefficient implies implies a positive correlation of PCT to the parameter (i.e., increasing PCT with increasing parameter value), whereas a negative coefficient implies a negative correlation (i.e., decreasing PCT with increasing parameter value). All maximum changes to PCT occur at 17 years decay time.

| Parameter | Sensitivity coefficient / rank | | | | | | Max. ΔPCT (°C) | |
|---|---|---|---|---|---|---|---|---|
| | 17 y | | 50 y | | 149 y | | | |
| Burnup ($\frac{\text{GWd}}{\text{MTU}}$) | 0.9088 | (1) | 0.7938 | (1) | 0.557 | (1) | 25.84 | (1) |
| Enrichment (% $^{235}$U) | -0.0483 | (4) | -0.0223 | (6) | -0.0292 | (7) | 12.39 | (2) |
| Moderator dens. ($\frac{\text{g}}{\text{cm}^3}$) | -0.146 | (2) | -0.238 | (2) | -0.432 | (2) | 5.17 | (3) |
| Moderator temp. (K) | 0.03 | (6) | 0.0206 | (7) | 0.0069 | (7) | 0.67 | (8) |
| Fuel temp. (K) | 0.0114 | (8) | 0.031 | (3) | 0.07 | (3) | 0.95 | (7) |
| Soluble boron (ppm) | 0.0185 | (6) | 0.0287 | (4) | 0.05 | (4) | 5.095 | (4) |
| WABA (Y/N) | 0.0117 | (7) | 0.0228 | (5) | 0.0444 | (5) | 4.32 | (5) |
| Pyrex (Y/N) | 0.109 | (3) | 0.0194 | (8) | 0.0367 | (6) | 3.66 | (6) |
| IFBA (Y/N) | 5.4E-4 | (9) | 3.2E-4 | (9) | 1E-5 | (9) | 0.15 | (9) |

The time dependence for each parameter's sensitivity coefficient indicates the evolution in the sensitivity contribution over time. For example, the increasing magnitude of the moderator density sensitivity coefficient over time (i.e., lower moderator density implies a higher PCT) can be explained by the increasing contribution of transuranic species to the total assembly decay heat over time, the production of which is tied directly to average moderator density.

*4.2. Cycle power history sensitivity*

In addition to an evaluation of the sensitivity of peak clad temperature to the irradiation history parameters, another relevant consideration is the effect of the final cycle specific power on the discharge decay heat over time. Here, given the fact that the equilibrium production rate of both fission product and TRU species is contingent upon the specific power, the discharge decay heat over time can likewise be linked to the specific power of the final irradiation cycle.

In order to consider the effect of the specific power (expressed in $\frac{\text{MW}}{\text{MTU}}$) of the final irradiation cycle on the discharge decay heat in isolation of the discharge burnup, here the burnup is preserved by simultaneously adjusting the specific power of the first two powers accordingly. For example, a 30% increase in the final cycle specific power is offset by a 15% reduction in the specific power of the first two cycles, and vice versa, thereby preserving the total burnup; this is illustrated as Figure 9.

The sensitivity of the decay heat relative to the change in the final cycle specific power is illustrated as Figure 10. One will immediately observe that unlike other cycle history parameters explored in the previous section, a

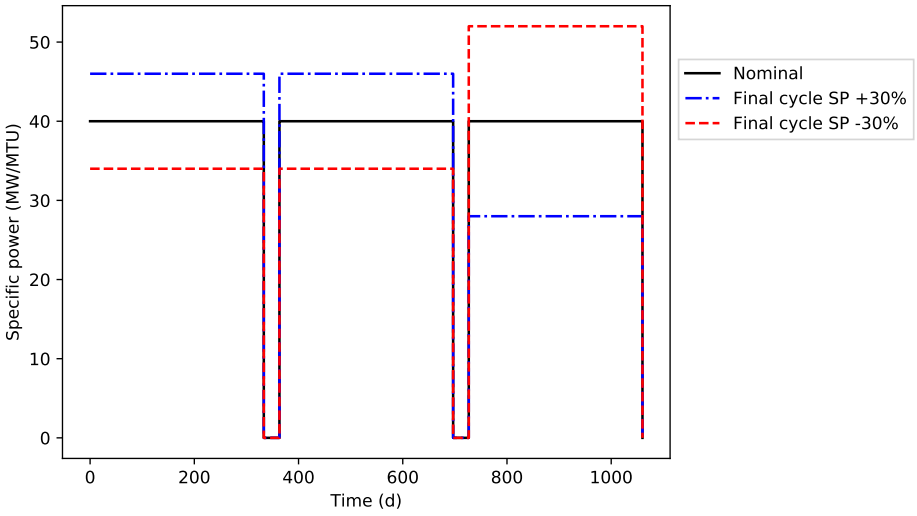


Figure 9: Example of specific power history perturbations considered for evaluating the impact of the last cycle specific power (in which assembly discharge burnup is preserved).

noticeable asymmetry exists between negative perturbations in the final cycle power (i.e., reductions in the final cycle power with a corresponding increase in the specific power of the first two cycles) and positive perturbations (i.e., increases in the final cycle specific power with a corresponding decrease in the specific power of the first two cycles). Here however the effect appears to be primarily confined to shorter decay periods (i.e., 5 years and below), wherein a decrease in the final cycle specific power produces a lower equilibrium concentration of short-lived fission products, thereby decreasing discharge decay heat (and vice versa). This effect largely vanishes at longer decay times (i.e., at 17 years and above) due to the decay of the short-lived fission products.

Table 5 details the sensitivity coefficients for negative and positive perturbations of the final cycle specific power. With respect to modifications of

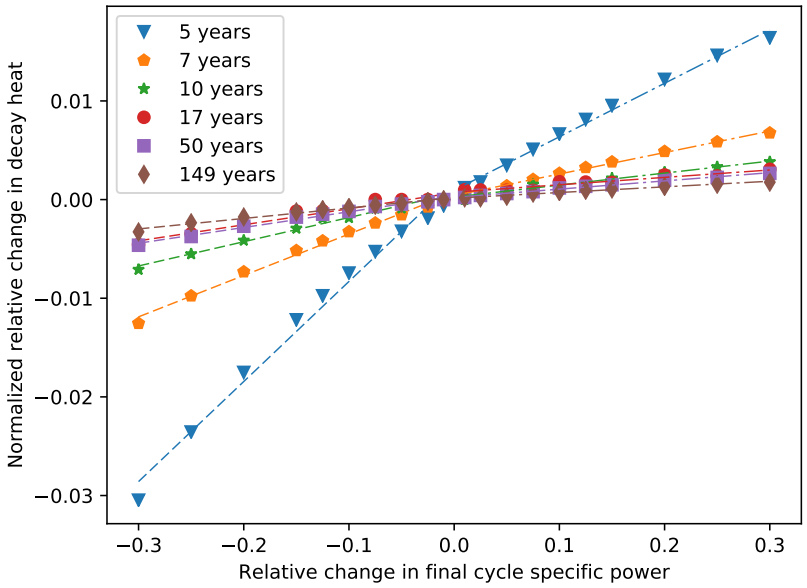


Figure 10: Sensitivity of assembly decay heat for different decay times based on relative perturbation of the final cycle specific power (wherein the specific powers of the first two cycles are subsequently adjusted to preserve total discharge burnup) for different assembly decay times. Dashed lines represent piecewise linear fits to the negative and positive perturbation domains.

the final cycle specific power, the decay heat sensitivity coefficients can be understood as follows: a 10% decrease in the final cycle specific power (along with a corresponding 5% increase in the specific power for the first two cycles) results in a 0.96% increase in decay heat at 5 years compared to the nominal case; a 0.14% increase in decay heat over nominal at 17 years decay time; a 0.15% increase in decay heat at 50 years decay time; and a 0.10% increase in decay heat over nominal at 149 years decay time. Conversely, the effect of a 10% increase in the final cycle specific power (and corresponding drop in the specific power of the first two cycles) results in a maximum increase of 0.5% in the decay heat, with the effect decreasing substantially over time as

Table 5: Decay heat sensitivity as a function of decay time for positive and negative perturbations of the final cycle specific power

| Decay time (y) | Final cycle perturbation (pos/neg) Negative | Positive |
|---|---|---|
| 5 | 0.101 | 0.054 |
| 7 | 0.042 | 0.022 |
| 10 | 0.025 | 0.012 |
| 17 | 0.016 | 0.008 |
| 50 | 0.016 | 0.008 |
| 149 | 0.011 | 0.006 |

short-lived fission products decay away.

To contextualize this result in terms of PCT response, a 10% change in discharge burnup from the nominal history (i.e., via a uniform 10% increase in the specific power in each cycle) results in a 10% change in decay heat at 17 and 50 years and a 12% increase in decay heat at 150 years. From Table 4, this corresponds to a 9.1% increase in PCT at 17 years post-discharge, a 7.9% increase in PCT at 50 years, and a 5.6% increase in PCT at 149 years decay time. Thus, the PCT sensitivity coefficient can be unfolded from the response to the change in final cycle specific power as follows:

$$\left(\frac{\delta PCT}{\delta SP}\right) = \left(\frac{\delta PCT}{\delta BU}\right) \cdot \left(\frac{\delta BU}{\delta DH}\right) \cdot \left(\frac{\delta DH}{\delta SP}\right) \tag{3}$$

In Equation 3, $\left(\frac{\delta PCT}{\delta BU}\right)$ is the sensitivity coefficient of PCT with respect to burnup, $\left(\frac{\delta BU}{\delta DH}\right)$ is inverse of the sensitivity coefficient of decay heat to burnup (i.e., fractional change in decay heat per unit change in burnup), and $\left(\frac{\delta DH}{\delta SP}\right)$ is the sensitivity of the decay heat to a unit change in final cycle specific power. In other words, given that the relationship of burnup to decay heat is

known and the relationship of burnup to PCT response is likewise known, by taking the decay heat response of the final cycle specific power, it is possible to therefore determine the sensitivity of PCT to decay heat. Using the values for the time-dependent PCT sensitivity coefficient for burnup from Table 5 yields the sensitivity coefficients for negative and positive perturbations in specific power, given as Table 6.

Table 6: PCT sensitivity coefficient as a function of decay time for positive and negative perturbations of the final cycle specific power $\left(\frac{\delta PCT}{\delta SP}\right)$

| Decay time (y) | Final cycle perturbation (pos/neg) Negative | Positive |
|---|---|---|
| 17 | 0.014 | 0.007 |
| 50 | 0.012 | 0.006 |
| 149 | 0.005 | 0.003 |

The sensitivity coefficient for the perturbation of the final cycle specific power (i.e., $\frac{\delta PCT}{\delta SP}$) can thus be interpreted as follows: a 10% decrease in the final cycle specific power (and a subsequent 5% increase in the specific power of the first two cycles) can be expected to produce a decrease in PCT of 0.14% at 17 years, 0.12% at 50 years, and 0.05% at 149 years decay time; similarly, a 10% increase in final cycle specific power would produce a 0.7% increase in PCT at 17 years post-discharge, 0.6% increase at 50 years decay time, and a 0.3% increase in PCT at 149 years decay time. Based on this finding, for longer cooling periods (i.e., over 5–7 years post-discharge), the specific distribution of the power history appears to be a negligible factor for best-estimate evaluation of PCT; rather, accurate estimation of the burnup and accommodation of other features that influence the neutron spectrum (e.g., the average moderator density) dominate the sensitivity of the decay heat

source term. While specific power history may be important for material studies for assemblies loaded into the cask following shorter pool storage times (i.e., under expedited removal schedules, given the higher decay heat during loading and drying), for assemblies stored in the pool for over 10 years, the effect of specific power history becomes negligible.

*4.3. Cask Model Sensitivity*

Many assumptions are used in the cask models, and some of these assumptions have been discussed in the description of the best-estimate thermal model for the MAGNASTOR® TSC-37 cask. To determine the impact of these assumptions on temperature predictions, these parameters are tested for PCT sensitivity by using a range of values that correspond to the uncertainty of that parameter or the variability that occurs in typical storage conditions, shown in Table 7.

An assembly total decay heat of 959 W equivalent to a total heat load per dry cask of 35.5 kW was used in the COBRA-SFS model sensitivity analysis. This heat load is the license limit heat capacity that can be loaded using the uniform decay heat loading pattern that was assumed in the base-case model. This decay heat corresponds to 2.3 wt% $^{235}$U W1515WL fuel that has a burnup of 40 $\frac{\text{GWd}}{\text{MTU}}$ and cooled for 7 years. Using the limiting cask heat loading for the sensitivity study affords an evaluation of the importance of fuel and cask design parameters during the most limiting period of storage (i.e., in which PCT is closest to the licensed limit). While using lower heat loading for the sensitivity study would lower the maximum difference in PCT, the respective sensitivity coefficients should remain the same.

Several parameters used in Table 7 are derived from those found in the

Table 7: COBRA-SFS modeling parameters used for sensitivity analysis

| Sensitivity | Nominal | Minimum | Maximum |
|---|---|---|---|
| Burnup profile skewness | 1.029 | 0.791 | 1.282 |
| Cladding emissivity | 0.8 | 0.3 | 0.8 |
| Spacer grid losses | 2 | 0 | 100 |
| Shell-basket gap (inches) | 0.125 | 0.001 | 1 |
| Canister pressure (atm) | 7 | 1 | 7 |
| Thermal conductivity $\left(\frac{\text{Btu}}{\text{ft}\cdot\text{hr}\cdot^\circ\text{F}}\right)$ | 100 | 84.5 | 115.5 |
| Annulus pressure drop (psi) | 0.00707 | 0.00699 | 0.00826 |
| Ambient air temperature (°F) | 80 | -40 | 105 |
| Insolation (top) $\left(\frac{\text{W}}{\text{m}^2}\right)$ | 387.75 | 0 | 387.75 |
| Insolation (side) $\left(\frac{\text{W}}{\text{m}^2}\right)$ | 193.9 | 0 | 193.9 |
| Basket emissivity | 0.8 | 0.3 | 0.8 |

MAGNASTOR® FSAR (NAC International, 2015). For example, the design basis for the MAGNASTOR® canister includes a helium backfill at 7 atm pressure (comprising the nominal and maximum pressure conditions); a minimum case of 1 atm is considered to evaluate the condition of a leak within the canister (wherein the pressure would slowly equalize to atmospheric pressure, i.e. 1 atm). Similarly, the FSAR assumes a nominal average ambient temperature of 80 °F, used as the nominal value here; the extreme three-day average temperatures of -40 and 105 °F are used in the FSAR to represent the lowest and highest off-normal temperatures (NAC International, 2015) and thus are used as the bounds of the sensitivity analysis here.

Meanwhile, the average insolation used from the top and side of the overpack derives from guidance in 10 CFR 71 §71 (U.S. Nuclear Regulatory Commission, 2017), the bounding value which is likewise used in the FSAR analysis (NAC International, 2015). Notably, this insolation estimate is it-

self conservative and bounding for all ISFSI locations; estimates from the National Renewable Energy Laboratory (NREL) indicate that the insolation for the continental United States is less than half that of the base-case assumption (National Renewable Energy Laboratory (NREL), 2014). For example, at the Zion nuclear power plant (where the MAGNASTOR® system is currently employed), the average daily insolation is 159.0 $\frac{\mathrm{W}}{\mathrm{m}^2}$ $\left(50.4\ \frac{\mathrm{Btu}}{\mathrm{h-ft}^2}\right)$ (National Renewable Energy Laboratory (NREL), 2014). For this analysis, the insolation sensitivity coefficient was evaluated by estimating the peak clad temperature with the bounding insolation values on the cask top and side and with insolation completely neglected.

With respect to the burnup profile, while a nominal skewness of 1.029 was used (i.e., a relatively symmetric burnup profile), bounding bottom-heavy (0.791) and top-heavy profiles (1.282) were chosen based on the most bounding profiles in the Caccapotui database (Cacciapouti and Volkinburg, 1997) to evaluate the sensitivity of peak clad temperature to the relative skewness of the burnup profile. Here, skewness is defined as the ratio of power produced in the top half of the assembly to that in the bottom half. Burnup profile skewness is expected to influence the rate of natural convection flow; i.e., a top-heavy profile would produce a lower flow rate than a bottom-heavy one due to the reduced buoyancy force. One caveat is that the analysis of the sensitivity of profile skewness is somewhat contrived when holding other assembly irradiation parameters (such as burnup) constant, given the inextricable link between burnup and profile shape; i.e., the profile skewness was varied while holding the total assembly decay heat constant at 959 kW. Nonetheless this analysis serves an illustrative purpose to demon-

strate the relative sensitivity of PCT relative to other cask and fuel assembly parameters.

The most significant variations in PCT in COBRA-SFS modeling parameters are for fill-gas pressure, annulus pressure head, ambient air temperature, and decay heat profile, as observed in Fig. 11. Over the range of parameters investigated, the maximum variations in PCT and corresponding sensitivity coefficients are provided in Table 8. Note here that due to the extreme ranges considered for certain parameters (such as the ambient air temperature and canister fill gas pressure), $\Delta$PCT is not provided, given that direct comparisons over these ranges are less meaningful than comparison of the relative sensitivity coefficients.

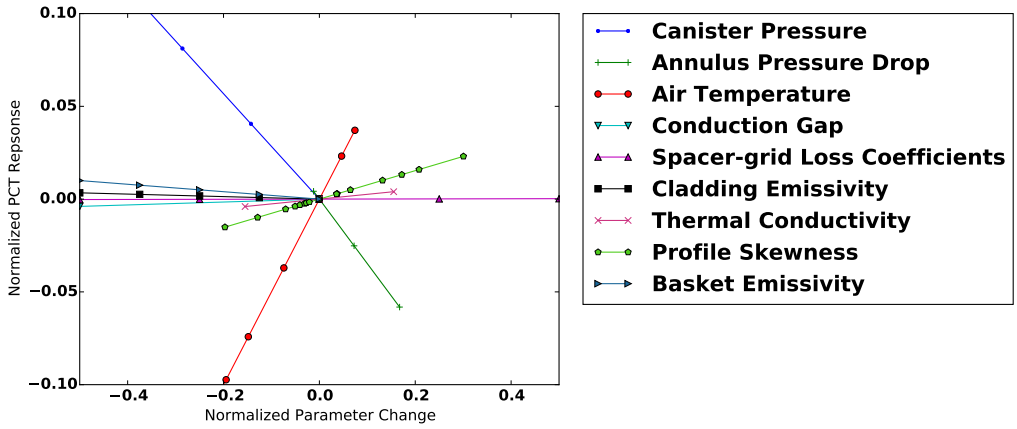


Figure 11: Peak clad temperature sensitivity to cask model parameters

The results confirm that as expected, peak clad temperature predictions are most sensitive to the modeling specifications that determine convective heat transfer properties in the basket and annulus. In particular, the ambient air temperature sensitivity coefficient exhibits a relatively large positive slope compared to other parameters, indicating an increase in PCT with

increasing ambient air temperature (and conversely, decreasing PCT with decreasing ambient air temperature). This relationship is intuitively obvious in that the canister heat removal is dominated by natural convection (and thus higher temperature gradients, such as due to lower ambient air temperatures, will drive convection), however the relative sensitivity of ambient air temperature compared to other parameters is especially notable, implying that local temperature cannot be ignored when developing best-estimate thermal models.

Table 8: COBRA-SFS modeling sensitivity results summary, including sensitivity coefficients for modeling parameters (for PCT) and rank-ordering of absolute sensitivity (1 = maximum sensitivity). Note that a positive sensitivity coefficient implies implies a positive correlation of PCT to the parameter (i.e., increasing PCT with increasing parameter value), whereas a negative coefficient implies a negative correlation (i.e., decreasing PCT with increasing parameter value).

| Parameter | Sensitivity coefficient | Rank |
|---|---|---|
| Ambient air temperature | 0.50 | (1) |
| Annulus pressure drop | -0.3477 | (2) |
| Canister pressure | -0.2841 | (3) |
| Burnup profile skewness | 0.0767 | (4) |
| Thermal conductivity | 0.0258 | (5) |
| Basket emissivity | -0.02 | (6) |
| Shell-basket gap | 0.0079 | (7) |
| Cladding emissivity | -0.0068 | (8) |
| Insolation (top + side) | 0.00244 | (9) |
| Spacer grid losses | 0.0004 | (10) |

Conversely, the canister fill gas pressure sensitivity coefficient shows a large, negative slope, translating into an overall increase in PCT with decreasing canister fill gas pressure (and vice versa). Here again the explanation is physically intuitive in that the density of the internal convection medium

(proportional to the pressure of the fill gas) drives the rate of convection from the fuel assemblies to the canister wall. While the fill gas pressure is not expected to be highly variable, its high sensitivity would indicate that even small deviations from nominal (due to leakage or other factors) can contribute significantly to PCT.

The pressure drop across the annular region likewise exhibits a negative sensitivity coefficient of roughly the same magnitude as the canister fill gas pressure, implying that the PCT will decrease with an increasing pressure drop. Physically, this pressure drop corresponds to the difference in the density of air between the inlet and the plenum region (refer to Equation 2), thus driving natural convection. Thus, as the pressure drop increases, buoyancy-driven flow likewise increases, increasing the rate of heat removal from the canister surface and lowering PCT. Here again it must be noted that the annulus pressure drop is not totally independent of the ambient air temperature, given the dependence of the inlet air density on ambient temperature; this however further underscores the need for capturing accurate local ambient environmental conditions for developing best-estimate thermal models.

Finally, the sensitivity coefficient corresponding to fuel burnup profile axial skewness also exhibits a moderate positive slope, indicating that for assemblies where decay heat is more concentrated toward the top of the fuel, natural convection is less effective at removing heat from the assemblies, whereas the opposite is true for bottom-heavy decay heat profiles.

Loss coefficients within the basket would be expected to have a significant effect on PCT, but the data shows little support for this. Radiative heat transfer from the basket external support structure to the canister plays a

very important role in heat removal. The cladding emissivity had very little effect on PCT over the very broad range of values used. Parameters that affected conduction had very little impact on PCT, though conduction in the basket provides a large surface area for convection. Meanwhile owing to the thermal isolation of the canister from the outside environment, insolation has a very small effect on PCT, with a difference of less than 1 °C arising from entirely neglecting insolation (as compared to the base-case bounding estimate of insolation intensity).

### *4.4. Effect of radiative transport*

A discussion of factors influencing best-estimate cask thermal model sensitivity would be incomplete without considering the effect of neglecting radiative heat transport mechanisms. Here the analysis will primarily focus on evaluation of the (conservative) error introduced by neglecting radiative heat transfer pathways. A comparison of the PCT change relative to a base case evaluation (with all radiative heat transfer pathways evaluated) is presented as Table 9.

Table 9: Changing in PCT resulting from omission of selected radiative heat transfer modeling pathways, compared to a baseline case with all radiative transport pathways evaluated (with a PCT of 364.8 °C).

| Pathways neglected | Δ PCT (°C) | Difference from nominal (%) |
|---|---|---|
| All (no radiation) | +118.6 | 18.59 |
| Basket-to-canister | +107.3 | 16.82 |
| Rod-to-rod and rod-to-basket | +7.4 | 1.16 |
| Annulus (canister-to-overpack) | +30.3 | 4.75 |

As is evident from Table 9, radiation from the fuel basket support struc-

ture to the canister wall is extremely significant and cannot be reasonably neglected. Similarly, neglecting radiative transport from the canister wall to the concrete overpack (i.e., within the annular region) raises the PCT estimate by about 4.8%, again indicating that contributions of radiative transport are non-trivial for this region; this finding is consistent with reported analysis in the MAGNASTOR® FSAR (NAC International, 2015).

Conversely, radiative transfer between individual rods and the fuel basket region is not a particularly significant pathway for heat removal, wherein neglecting this pathway leads to a 1.2% increase in PCT. This latter result is attributable to the fact that the emissivity of the cladding and the carbon-steel basket are both modeled with the same emissivity value (0.8); as a result, head radiated to the basket is almost entirely radiated back to the pins. However, as is shown in Table 8, the basket emissivity has a comparably low effect on PCT, indicating that radiative transport is not the dominant transport mechanism from the fuel within the basket.

## 5. Discussion

### *5.1. Influence of factors impacting decay heat on PCT sensitivity*

Of all of the factors influencing PCT sensitivity, fuel assembly irradiation history parameters that drive decay heat are dominant. This is not a surprising conclusion, given that factors such as the discharge burnup can have a profound effect upon decay heat. However, apart from factors such as the discharge burnup, average moderator density, and the initial enrichment, many irradiation history parameters are of relatively small influence on PCT.

Factors that increase the fast neutron flux tend to be the most sensitive

because of the increase in neutron absorption probability in $^{238}$U, leading to increased minor actinoid concentration. The most sensitive parameters are moderator density and burnable absorber rod insertion (both of which directly influence the thermal neutron flux), which have sensitivity coefficients of 0.432 and 0.0444 at a cooling time of 150 years, respectively. If uncertainty in burnup measurements were as high as tested with roughly 5% uncertainty, then burnup would be the most sensitive parameter. The maximum sensitivity coefficient for burnup is 0.9088 at an early cooling time of 15 years, resulting in a difference in PCT of 26 °C. PCT is most sensitive to burnup at short cooling times because the fission product concentration is proportional to burnup, and fission products are the dominant decay heat source from immediately after discharge up to about 50 years of cooling time.

Decay heat predictions using known enrichment and burnup values show the variability in reactor operating history has little effect on PCT. In particular, effects owing to the specific power history (i.e., the distribution of the last cycle power relative to other cycles) are negligible for storage times over 5–7 years, producing extremely small changes to PCT, with effects comparable to those of the average moderator temperature. While such an effect can be expected to be important for material studies involving expedited removal of assemblies from the storage pools, for assemblies stored in the pool for a decade or more, the effect of specific power history is of negligible importance. In as much, coarser estimates (e.g., uniform cycle powers) may be employed for best-estimate thermal models under these conditions without a substantial loss in accuracy. Meanwhile, other factors such as the presence of burnable poisons and soluble boron levels are second-order contributors

to decay heat sensitivity with effects manifesting primarily at very long storage times due to their influence over the neutron spectrum (and thus TRU production).

*5.2. Impact of factors influencing convection-driven flow on PCT sensitivity*

Of the most significant parameters affecting PCT outside of those factors that drive the decay heat source term are those that have a direct influence on convective heat transport. The parameters in this study that fall into this category within the cannister are decay heat profile (i.e., the relative skewness of the decay heat generated over the axial profile of the assembly), spacer grid losses within the basket, and the canister gas backfill pressure. Both the decay heat profile and canister pressure had considerable impact on PCT with sensitivity coefficients of 0.0767 and -0.2841, respectively. The canister pressure is the more sensitive of the two because the decrease in pressure changes the thermo-physical properties of the back-fill helium gas.

In particular, the significant influence of the burnup profile shape on PCT arises due to the axial distribution of the heat flux in the canister, influencing natural circulation rates. More heat concentrated towards the top of the canister decreases flow in the canister by shifting the low density air towards the top of the canister, thereby decreasing the buoyancy force on the gas. This has direct implications to cask thermal analyses that utilize multiple axial zones to determine total assembly fissile content. Over a period of 100 years, the dominant decay heat contributors change from fission products to mainly actinoids (as the dominant fission product species that drive decay heat–$^{137}$Cs and $^{90}$Sr–decay away), which are produced in higher concentrations towards the top of the fuel because of the lower moderator density,

higher fuel temperature, and effects from control rod insertion—all of which increase the production of minor actinoids. These effects could flip the profile shape over time and lead to considerable differences in PCT predictions. Using specific cross-section libraries for each axial zone captures the effect of spectrum differences and better simulates the change in profile shape over time than using a single cross-section library for all axial zones.

Spacer grid losses within the basket however exhibited the lowest sensitivity of all parameters considered, with a sensitivity coefficient of 0.0004, implying very small upward changes in PCT in response to increases in frictional flow losses from the spacer grid. While spacer grid pressure losses are significant source of uncertainty in cask models, this analysis shows that overall peak clad temperatures show minimal sensitivity to this factor, likely due to laminar fluid flow of the helium gas in dry storage conditions (NAC International, 2015). This parameter would therefore be an example of a high uncertainty / low-sensitivity parameter of minimal consequence to overall best-estimate thermal model uncertainty. Analysts can thus safely assume a nominal value for spacer grid drag losses with minimum consequence to model fidelity for best-estimate thermal models.

Flow in the annulus region between the canister and overpack is critical to heat removal, and PCT was very sensitive to parameters that affect this region. These parameters are the annulus pressure drop and ambient air temperature. Both of these parameters determine the flow rate through the annulus region of the storage overpack by directly varying the pressure drop across the annulus or by changing the density of the ambient air that is used to calculate the pressure drop. The sensitivity coefficients for these param-

eters are -0.3477 for the annulus pressure drop and 0.50 for the ambient air temperature. These two parameters are highly correlated in that a change in the ambient air temperature will also change the pressure drop across the annulus. Ambient air temperature has the most significant impact on PCT with a degree change in air temperature resulting in a proportional degree change in PCT. This is problematic for best-estimate thermal modeling because air temperature changes throughout the course of a day and average temperatures change throughout the year. Although the cask has a large thermal capacitance, the PCT is likely non-constant during typical storage conditions, fluctuating between maximum and minimum values. Thus, in addition to requiring specific information about site environmental conditions for best-estimate thermal models, the strong dependence on (inherently variable) ambient air temperature would imply a substantial inherent uncertainty in calculated PCT from best-estimate thermal models.

*5.3. Effects governing radiation and conduction*

Interestingly, material properties that influence radiative transport such as the emissivity of the cladding or basket structure had very little effect on PCT except for the region between the basket support structure and canister inner surface, with overall PCT sensitivity coefficients of -0.0068 and -0.02, implying relatively low sensitivity to these parameters. Limitations in calculating greybody view factors for the external support structure of the basket and canister inner surface may add some uncertainty to PCT results. Thermal conductivity and conduction between the basket structure and the canister shell likewise did not exhibit a significant impact on PCT; for example, the width of the shell-basket gap (offering a potential conduction pathway

from the fuel basket to the canister shell) gave a PCT sensitivity coefficient of 0.0079. These results support the hypothesis that the MAGNASTOR® canister system relies primarily on natural convection within the canister to transport heat from the fuel to the canister shell.

However, it is important to note that radiation is an extremely important heat removal pathway from the basket support structure (surrounding the fuel baskets) and the cannister wall, the neglect of which can lead to profound overestimation of PCT (up to about 17%). Additionally, radiation from the canister wall to the overpack is a significant non-dominant contributor to heat removal. While PCT shows little sensitivity to material properties governing radiative transport (such as emissivity), the radiation transport pathway in these two regions is nonetheless significant to best-estimate thermal models. Conversely, PCT is far less sensitive to radiative transport between the fuel rods and the fuel basket, indicating that radiative transport is not as significant to heat removal in this region.

## 6. Conclusions

In this paper, we have sought to characterize modeling parameters for vertical dry storage cask designs that show the greatest temperature sensitivity in order to aid in the development of best-estimate thermal models for used fuel storage. Due to the fact that material degradation processes such as hydride reorientation in zirconium-based cladding show a strong dependence on temperature (both in terms of clad temperature as well as thermal cycling and cool-down rates), best-estimate thermal models may prove more useful for understanding relevant potential cladding degradation mechanisms over

the course of long-term storage as compared to typical bounding analyses used for licensing. Identification of the most sensitive parameters for peak clad temperature can thus be used to inform best-estimate thermal model development, both in more precise estimation of uncertainties in peak clad temperatures as well as in identification of high-priority modeling parameters of both the fuel irradiation history, cask geometry (including relevant thermal hydraulic parameters), and ambient environmental conditions. To this end, a number of fuel-, cask-, and site-specific parameters have been shown to have important impacts on best-estimate predictions of the fuel thermal conditions during storage. In particular, this work has sought to place the sensitivity of well-understood thermal parameters (i.e., contributors to spent fuel decay heat) into a larger framework that likewise captures all relevant aspects of the dry storage system, including cask design parameters that have heretofore chiefly been modeled using more conservative bounding values for safety assessments.

Vertical storage casks rely on natural convection to the environment as the primary means for decay heat removal from the system. Some canisters (such as the MAGNASTOR® TSC-37) are designed to employ internal natural convection to remove heat from the fuel. Our findings indicate that modeling parameters that most strongly influence convective heat transport therefore have the greatest sensitivity for PCT estimates. The parameters in this study that fall into this category are the relative axial skewness of the decay heat profile, the canister gas backfill pressure, and spacer grid losses within the basket, the first two of which exhibit a strong influence on PCT. Spacer grid losses within the basket however exhibited the lowest sensitivity

of all parameters considered; this parameter would be an example of a high uncertainty / low-sensitivity parameter of minimal consequence to overall best-estimate thermal model uncertainty.

This study identified a number of system and modeling parameters that have a large impact on PCT predictions in vertical dry cask storage systems. Our findings indicate that the peak clad temperatures in vertical dry cask storage systems most sensitive to modeling parameters include irradiation parameters which drive the total decay heat in the stored fuel (such as the discharge burnup, distribution of cycle specific powers, and factors that influence spectrum hardness such as moderator density and soluble boron) as well as cask/fuel modeling parameters that influence natural convection rates, such as the pressure drop across the annulus region between the canister and overpack (i.e., the dominant heat removal pathway of the system), fill gas pressure, and the axial decay heat profile of the fuel. Additionally, the average ambient air temperature likewise has a strong influence on natural convection rates within the annular region. Conversely, properties which drive radiative heat transport (such as the emissivity of the cladding and fuel basket materials) had a relatively limited influence on PCT, implying convective factors dominate peak clad temperatures. Factors that influence conductive transport, such as the thermal conductivity of the basket and canister materials and the shell-basket gap had a moderate influence on PCT, but significantly less so than those that influence convection.

On the basis of these findings, we recommend that future work for best-estimate thermal models for vertical dry cask storage systems focus on accurate estimation the decay heat source term and factors that influence con-

vective transport, such as capturing the irradiation history of the assembly (including the discharge burnup, axial burnup profile, and average moderator density), the pressure drop across the annular region (governing buoyancy-driven flow), the canister fill gas pressure, and site-specific factors such as the average ambient air temperature. The latter of these properties is especially important to best-estimate thermal models, given the overall sensitivity of peak clad temperature to ambient air temperatures. In as much, the use of bounding values for ambient air temperature is clearly inappropriate for best-estimate models of peak clad temperature; here, the use of site-specific values is essential.

Conversely, factors driving radiative transport within the fuel basket (such as the cladding and fuel basket emissivity), and factors influencing conduction from the fuel basket (e.g., the thermal conductivity of the fuel basket and the shell-basket gap size) are of secondary importance for best-estimate thermal models. Finally, while factors such as solar insolation offer additional model conservatism, its effect on peak clad temperature (and the sensitivity thereof) is overall negligible.

An important caveat that these findings apply exclusively to vertical dry cask storage systems and particular canister designs; given the substantially different dominant heat removal mechanisms for horizontal dry storage cask systems, the conclusions from this study cannot be assumed to be directly translate to these systems, which would warrant a separate study.

## 7. Acknowledgments

This work has been supported by the DOE Office of Nuclear Energy. The authors also wish to express their appreciation to Henrik Liljenfeldt and Kaushik Banerjee of Oak Ridge National Laboratory for their thoughtful comments and feedback provided in preparing this paper.

## References

Office of Nuclear Material Safety and Safeguards, Standard Review Plan for Spent Fuel Dry Storage Systems at a General License Facility – Final Report, Technical Report NUREG-1536, Revision 1, U.S. Nuclear Regulatory Commission, 2010. URL: `https://www.nrc.gov/reading-rm/doc-collections/nuregs/staff/sr1536/r1/`.

K. B. Sorenson, B. Hanson, Making the Case for Safe Storage of Used Nuclear Fuel for Extended Periods of Time: Combining Near-Term Experiments and Analyses with Longer-Term Confirmatory Demonstrations, Nuclear Engineering and Technology 45 (2013) 421–426.

R. S. Daum, S. Majumdar, Y. Liu, M. C. Billone, Radial-hydride Embrittlement of High-burnup Zircaloy-4 Fuel Cladding, Journal of Nuclear Science and Technology 43 (2006) 1054–1067.

Y.-J. Kim, D.-H. Kook, T.-H. Kim, J.-S. Kim, Stress and temperature-dependent hydride reorientation of zircaloy-4 cladding and its effect on the ductility degradation, Journal of Nuclear Science and Technology 52 (2015) 717–727.

D. Kook, J. Choi, J. Kim, Y. Kim, Review of Spent Fuel Integrity Evaluation for Dry Storage, Nuclear Engineering and Technology 45 (2013) 115–124.

R. Singh, R. L. Mikin, G. Dey, D. Sah, I. Batra, P. Støahle, Influence of temperature on threshold stress for reorientation of hydrides and residual stress variation across thickness of Zr–2.5Nb alloy pressure tube, Journal of Nuclear Materials 359 (2006) 208 – 219.

S.-J. Min, J.-J. Won, K.-T. Kim, Terminal cool-down temperature-dependent hydride reorientations in Zr-Nb Alloy claddings under dry storage conditions, Journal of Nuclear Materials 448 (2014) 172–183.

H.-J. Cha, J.-J. Won, K.-N. Jang, J.-H. An, K.-T. Kim, Tensile hoop stress-, hydrogen content- and cooling rate-dependent hydride reorientation behaviors of Zr alloy cladding tubes, Journal of Nuclear Materials 464 (2015) 53–60.

H. Chu, S. Wu, R. Kuo, Hydride reorientation in Zircaloy-4 cladding, Journal of Nuclear Materials 373 (2008) 319–327.

K. B. Colas, A. T. Motta, M. R. Daymond, J. D. Almer, Effect of thermomechanical cycling on zirconium hydride reorientation studied in situ with synchrotron X-ray diffraction, Journal of Nuclear Materials 440 (2013) 586–595.

J.-J. Won, M.-S. Kim, K.-T. Kim, Heat-Up And Cool-Down Temperature-Dependent Hydride Reorientation Behaviors in Zirconium Alloy Cladding Tubes, Nuclear Engineering and Technology 46 (2014) 681–688.

S. Valance, J. Bertsch, Hydrides reorientation investigation of high burn-up PWR fuel cladding, Journal of Nuclear Materials 464 (2015) 371 – 381.

M. Billone, T. Burtseva, J. Dobrzynski, D. McGann, Z. H. K. Byrne, Y. Liu, Phase I Ring Compression Testing of High-Burnup Cladding, Technical Report FCRD-USED-2012-000039, Argonne National Laboratory, 2011. URL: http://www.ipd.anl.gov/anlpubs/2013/03/76043.pdf.

NAC International, MAGNASTOR Final Safety Analysis Report, Revision 7, Agencywide Documents Access and Management System (ADAMS) Accession No. ML16236A177, U.S. Nuclear Regulatory Commission, 2015. URL: https://adamswebsearch2.nrc.gov/webSearch2/view?AccessionNumber=ML16236A177, Docket No. 72-1031.

J. Scaglione, K. Banerjee, K. Robb, R. LeFebvre, The Used Nuclear Fuel Storage, Transportation, and Disposal Analysis Resource and Data System, in: Proceedings of the Institute of Nuclear Materials Management, 55th Annual Meeting, Atlanta, GA, 2014.

K. R. Robb, R. DeVoe, T. E. Michener, J. M. Scaglione, Thermal modeling capability development for as-loaded commercial used nuclear fuel casks, in: Transactions of the American Nuclear Society, volume 111, 2014, pp. 353–356.

S. M. Bowman, SCALE 6: Comprehensive Nuclear Safety Analysis Code System, Nuclear Technology 174 (2011) 126–148.

T. E. Michener, D. R. Rector, J. M. Cuta, H. E. Adkins, Jr., COBRA-SFS:

A Thermal-Hydraulic Analysis Code for Spent Fuel Storage and Transportation Casks, Cycle 4, Richland, Washington, 2015. PNNL-24841.

M. D. DeHart, S. M. Bowman, Reactor physics methods and analysis capabilities in SCALE, Nuclear Technology 174 (2011) 196–213.

I. C. Gauld, G. Radulescu, G. Ilas, B. D. Murphy, M. L. Williams, D. Wiarda, Isotopic depletion and decay methods and analysis capabilities in SCALE, Nuclear Technology 174 (2011) 169–195.

I. C. Gauld, G. Illas, B. D. Murphy, C. F. Weber, Validation of SCALE 5 Decay Heat Predictions for LWR Spent Nuclear Fuel, Technical Report NUREG/CR-6972, Oak Ridge National Laboratory, 2010.

G. Radulescu, I. Gaud, G. Ilas, SCALE 5.1 Predictions of PWR Spent Nuclear Fuel Isotopic Compositions, Technical Report ORNL/TM-2010/44, Oak Ridge National Laboratory, 2010.

S. E. Skutnik, M. L. Williams, R. A. Lefebvre, ORIGAMI: A new interface for fuel assembly characterization with ORIGEN, in: 2015 International High-Level Radioactive Waste Management Conference, 2015, pp. 418–425.

S. Skutnik, F. Havlůj, D. Lago, I. Gauld, Development of an Object-Oriented ORIGEN for Advanced Nuclear Fuel Modeling Applications, in: International Conference on Mathematics and Computational Methods Applied to Nuclear Science & Engineering (M&C 2013), Sun Valley, ID, 2013.

W. A. Wieselquist, The SCALE 6.2 ORIGEN API for High-Performance

Depletion, in: Joint International Conference on Mathematics and Computation (M&C), Supercomputing in Nuclear Applications (SNA) and the Monte Carlo (MC) Method (M&C 2015), 2015.

H. E. Adkins Jr., J. M. Cuta, B. J. Koeppel, A. D. Guzman, C. S. Bajwa, Spent Fuel Transportation Package Response to the Baltimore Tunnel Fire Scenario, Agencywide Documents Access and Management System (ADAMS) Accession No. ML062340334 NUREG/CR-6886, Pacific Northwest National Laboratory, 2009.

C. S. Bajwa, I. F. Spivack, Benchmarking of a thermal finite element approximation scheme for externally cooled spent fuel storage casks, in: ASME 2007 Pressure Vessels and Piping Conference, 2007.

C. Greene, StoreFUEL and Decommissioning Report, volume 16, Ux Consulting Company LLC, 2015.

G. Radulescu, D. E. Mueller, J. C. Wagner, Sensitivity and Uncertainty Analysis of Commercial Reactor Criticals for Burnup Credit, Technical Report NUREG/CR-6951, Oak Ridge National Laboratory, 2008.

Office of Civilian Radioactive Waste Management, Characteristics of spent fuel, high-level waste, and other radioactive wastes which may require long-term isolation, Rev. 0, Technical Report DOE/RW-0184, U. S. Department of Energy, 1987. URL: https://curie.ornl.gov/content/characteristics-spent-fuel-high-level-waste-and-other-radioactive-wastes-which-may-require.

R. J. Cacciapouti, S. V. Volkinburg, Axial Burnup Profile Database for Pressurized Water Reactors, Technical Report YAEC-1937, Yankee Atomic Electric Company, 1997.

U.S. Nuclear Regulatory Commission, Packaging and Transportation of Radioactive Material, 2017. URL: http://www.nrc.gov/reading-rm/doc-collections/cfr/part071.

National Renewable Energy Laboratory (NREL), 10-kilometer solar data spreadsheet, direct normal insolation data, 2014. URL: http://www.nrel.gov/gis/docs/SolarSummaries.xlsx, retrieved: December 2016.